The Astrophysical Journal, 777:36 (12pp), 2013 November 1 doi:10.1088/0004-637X/777/1/36

THE EXEMPLAR T8 SUBDWARF COMPANION OF WOLF 1130

Gregory N. Mace[1,2], J. Davy Kirkpatrick[2], Michael C. Cushing[3], Christopher R. Gelino[2], Ian S. McLean[1], Sarah E. Logsdon[1], Edward L. Wright[1], Michael F. Skrutskie[4], Charles A. Beichman[2], Peter R. Eisenhardt[5], and Kristin R. Kulas[1]

[1] Department of Physics and Astronomy, UCLA, 430 Portola Plaza, Box 951547, Los Angeles, CA 90095-1547, USA; gmace@astro.ucla.edu
[2] Infrared Processing and Analysis Center, MS 100-22, California Institute of Technology, Pasadena, CA 91125, USA
[3] Department of Physics and Astronomy, MS 111, University of Toledo, 2801 W. Bancroft St., Toledo, OH 43606-3328, USA
[4] Department of Astronomy, University of Virginia, Charlottesville, VA 22904, USA
[5] NASA Jet Propulsion Laboratory, 4800 Oak Grove Drive, Pasadena, CA 91109, USA

Received 2013 July 1; accepted 2013 September 5; published 2013 October 11

ABSTRACT

We have discovered a wide separation (188.″5) T8 subdwarf companion to the sdM1.5+WD binary Wolf 1130. Companionship of WISE J200520.38+542433.9 is verified through common proper motion over a ∼3 yr baseline. Wolf 1130 is located 15.83 ± 0.96 pc from the Sun, placing the brown dwarf at a projected separation of ∼3000 AU. Near-infrared colors and medium resolution ($R \approx 2000$–4000) spectroscopy establish the uniqueness of this system as a high-gravity, low-metallicity benchmark. Although there are a number of low-metallicity T dwarfs in the literature, WISE J200520.38+542433.9 has the most extreme inferred metallicity to date with [Fe/H] = −0.64 ± 0.17 based on Wolf 1130. Model comparisons to this exemplar late-type subdwarf support it having an old age, a low metallicity, and a small radius. However, the spectroscopic peculiarities of WISE J200520.38+542433.9 underscore the importance of developing the low-metallicity parameter space of the most current atmospheric models.

Key words: binaries: general – brown dwarfs – stars: individual (Wolf 1130, WISE J200520.38 + 542433.9) – stars: low-mass

Online-only material: color figures

1. INTRODUCTION

The sample of known T dwarfs has grown considerably since the discovery of Gl 229B (Nakajima et al. 1995). The bulk of the sample has been revealed through surveys like the Two Micron All Sky Survey (2MASS; Skrutskie et al. 2006), the Sloan Digital Sky Survey (SDSS; York et al. 2000), the United Kingdom Infrared Telescope Infrared Deep Sky Survey (UKIDSS; Lawrence et al. 2007), the Canada France Hawaii Telescope Legacy Survey (CFHTLS; Delorme et al. 2008), and the *Wide-field Infrared Survey Explorer* (*WISE*; Wright et al. 2010). Constraining physical properties like mass, age, and metallicity for isolated field brown dwarfs discovered by such surveys inevitably requires comparison to models. These models are improved by employing wide-separation T dwarf companions to well studied stars as benchmarks for our analysis of the larger solivagant population (Burgasser et al. 2000, 2005; Wilson et al. 2001; Scholz et al. 2003; McCaughrean et al. 2004; Mugrauer et al. 2006; Liu et al. 2007; Luhman et al. 2007; Pinfield et al. 2006, 2008, 2012; Burningham et al. 2009, 2013; Goldman et al. 2010; Albert et al. 2011; Day-Jones et al. 2011; Luhman et al. 2011; Murray et al. 2011; Deacon et al. 2012a, 2012b; Dupuy & Liu 2012; Wright et al. 2013).

WISE J200520.38+542433.9 (WISE 2005+5424 hereafter) is a faint ($J \sim 19.6$ mag), late-type T dwarf located 188.″5 from Wolf 1130 in the constellation Cygnus. Wolf 1130 (LHS 482, Gl 781) is a well constrained high-proper motion system (van Leeuwen 2007) at ∼16 pc from the Sun. Additionally, Wolf 1130 has been identified as a ∼12 hr period single-lined spectroscopic binary consisting of a M1.5 subdwarf and possibly a helium white dwarf (Gizis 1998). UVW space velocities in the literature identify Wolf 1130 as a member of the old disk or halo population (Stauffer & Hartmann 1986; Leggett 1992), and Rojas-Ayala et al. (2012) determine a low metallicity ([Fe/H] = −0.64 ± 0.17 dex) for the M1.5 subdwarf component of the system. All of these characteristics imply an age of at least 2 Gyr for Wolf 1130 (Hansen & Phinney 1998), but more likely 10–15 Gyr.

In this paper we present the discovery of the T8 subdwarf WISE 2005+5424. Astrometry from space- and ground-based imaging verifies this object as having a common proper motion with Wolf 1130. We have compiled photometry and near-infrared spectroscopy of WISE 2005+5424 that show the hallmarks of low metallicity and advanced age. In Section 2 we describe our imaging and photometry, while Section 3 describes the spectroscopic observations. Analysis of our observations is presented in Section 4 and the primary properties of WISE 2005+5424 are summarized in Section 5.

2. IMAGING AND PHOTOMETRY

WISE 2005+5424 was selected as a brown dwarf candidate by employing the WISE All-Sky Data Release (Cutri et al. 2012) color selection criteria described by Kirkpatrick et al. (2011, 2012) and Mace et al. (2013). Tables 1 and 2 list various parameters for Wolf 1130 and WISE 2005+5424 from the literature and the analysis in this paper. Figure 1 shows a compilation of images centered on WISE 2005+5424, which is too faint to be detected in the 2MASS survey and lies outside the UKIDSS Galactic Plane Survey area (Lawrence et al. 2007; Lucas et al. 2008).

2.1. 2MASS

Photometry for Wolf 1130 is from the 2MASS All-Sky Point Source Catalog. In the 2MASS images Wolf 1130 is ∼6″ away from a background source. *J*- and *H*-band measurements were unblended and derived with a single component fit.

Table 1
Properties of Wolf 1130 and WISE 2005+5424

	Wolf 1130	WISE 2005+5424
α_{WISE} (J2000)	$20^h05^m00^s.82$	$20^h05^m20^s.38$
δ_{WISE} (J2000)	$+54^d25^m53^s.9$	$+54^d24^m33^s.9$
l_{WISE}(deg)	88.5821686	88.5870493
b_{WISE} (deg)	11.9790854	11.9269303
$W1$ (mag)	7.952 ± 0.023	18.819 ± 0.536[a]
$W2$ (mag)	7.800 ± 0.020	14.941 ± 0.057
$W3$ (mag)	7.726 ± 0.017	>12.973
$W4$ (mag)	7.613 ± 0.089	>9.07
$W1-W2$ (mag)	0.152 ± 0.030	3.878 ± 0.539
$W2-W3$ (mag)	0.074 ± 0.026	<1.968
$ch1$ (mag)	...	15.870 ± 0.028
$ch2$ (mag)	...	14.625 ± 0.020
$ch1-ch2$ (mag)	...	1.245 ± 0.034
J_{MKO} (mag)	...	19.640 ± 0.089
H_{MKO} (mag)	...	19.572 ± 0.079
J_{2MASS} (mag)	8.830 ± 0.021	...
H_{2MASS} (mag)	8.346 ± 0.021	...
Ks_{2MASS} (mag)	8.113 ± 0.018	...
$(J-H)_{MKO}$ (mag)	...	0.068 ± 0.119
$J_{MKO}-W2$ (mag)	...	4.699 ± 0.106
$H_{MKO}-W2$ (mag)	...	4.631 ± 0.097
μ_α (arcsec yr^{-1})	-1.163 ± 0.005[b]	-1.138 ± 0.102
μ_δ (arcsec yr^{-1})	-0.900 ± 0.004[b]	-0.988 ± 0.106
π (mas)	63.17 ± 3.82[b]	19 ± 96
d (pc)	15.83 ± 0.96	...
γ (km s^{-1})	-34[c]	...
U (km s^{-1})[d,e]	-101 ± 7	...
V (km s^{-1})[e]	-44 ± 2	...
W (km s^{-1})[e]	33 ± 3	...
M_H (mag)	...	18.57 ± 0.21
M_{W2} (mag)	...	13.94 ± 0.19
T_{eff} (K)	3483 ± 17[f]	600–900
[M/H] (dex)	-0.45 ± 0.12[f]	...
[Fe/H] (dex)	-0.64 ± 0.17[f]	...

Notes.
[a] SNR = 2, the limit for profile-fit magnitude uncertainties.
[b] van Leeuwen (2007).
[c] Gizis (1998).
[d] U velocity is positive away from the Galactic center.
[e] Space motions are relative to the Sun and not the local standard of rest.
[f] Rojas-Ayala et al. (2012).

The K_s-band photometry for Wolf 1130 required a two component fit to deblend it from the neighboring source.

2.2. WISE

The *WISE* mission was a two-pass all-sky survey at 3.4, 4.6, 12, and 22 μm, hereafter referred to as bands W1, W2, W3, and W4, respectively (Wright et al. 2010). WISE 2005+5424 was identified by its red $W1-W2$ and $W2-W3$ colors. As a variant of the methane imaging technique, redder $W1-W2$ colors identify a lack of flux in the deep 3.3 μm CH_4 absorption band relative to the abundant 4.6 μm flux in T and Y dwarfs (Rosenthal et al. 1996; Tinney et al. 2005; Wright et al. 2010; Mainzer et al. 2011).

Figure 2 shows the $W1-W2$ and $W2-W3$ colors of WISE 2005+5424 along with other *WISE*-discovered T and Y dwarfs. The $W1-W2$ color of WISE 2005+5424 is consistent with a type later than T6. The $W2-W3$ color is an upper limit and is not a useful independent indicator of the object's expected spectral type, but the limit is consistent with a T or Y dwarf. The two *WISE* epochs used in our astrometric solution are from the All-Sky Data Release for the first *WISE* epoch and the average of the twenty detections in the Post-Cryo Single Exposure Source Table for the second *WISE* epoch.

2.3. Spitzer

The Infrared Array Camera (IRAC; Fazio et al. 2004) on board the *Spitzer Space Telescope* (Werner et al. 2004) was used during the warm *Spitzer* mission to obtain deeper, more precise photometry of WISE 2005+5424 in the 3.6 and 4.5 μm channels (hereafter, $ch1$ and $ch2$, respectively). Observations were made on three separate epochs as part of Cycle 7 and Cycle 8 programs 70062 and 80109 (Kirkpatrick, PI). Data acquisition and reduction was the same as in Kirkpatrick et al. (2011) and Mace et al. (2013). The $ch1-ch2$ color as a function of spectral type is shown in Figure 3. This *Spitzer* photometry constrains WISE 2005+5424 to spectral types between T5 and T8, which is a narrower range than the *WISE* colors imply. The $ch1-ch2$ versus $W1-W2$ color–color diagram is also shown in Figure 3. WISE 2005+5424 occupies a unique corner of this color space, which we discuss in more detail in Section 4.3.

2.4. WIRC

Photometry of WISE 2005+5424 on the MKO system (Simons & Tokunaga 2002; Tokunaga et al. 2002) is from the Wide-field Infrared Camera (WIRC; Wilson et al. 2003) at the 5 m Hale Telescope at Palomar Observatory. Source extractions from our observations use apertures that are 1.5 × FWHM of the source point-spread function following the method outlined by Kirkpatrick et al. (2011). The MKO $J-H$ colors for a collection of objects from the literature (Leggett et al. 2010a, 2012, 2013; Albert et al. 2011; Kirkpatrick et al. 2011, 2012; Dupuy & Liu 2012; Mace et al. 2013; Burningham et al. 2010b, 2013; Thompson et al. 2013) are shown in Figure 4. WISE 2005+5424 is redder in $J-H$ than the T5–T8 spectral type constrained by *Spitzer* and mostly consistent with late-type T dwarfs. The red

Table 2
Astrometric Measurements of WISE 2005+5424

Facility/ Instrument	MJD JD−2400000.5	R.A. (deg)	$\sigma_{R.A.}$ (arcsec)	Decl. (deg)	$\sigma_{Decl.}$ (arcsec)
WISE All-Sky	55343.731516	301.3349418	0.378	+54.4094230	0.382
WISE Post-Cryo	55524.165	301.334676	0.38	+54.409242	0.38
Spitzer/IRAC	55561.659165	301.3346646	0.183	+54.4093114	0.165
Spitzer/IRAC	55748.962883	301.3344610	0.198	+54.4091562	0.226
Spitzer/IRAC	55886.077227	301.3342873	0.151	+54.4090573	0.230
Palomar/WIRC	56137.837095	301.3338706	0.19	+54.4089008	0.22
Keck/NIRSPEC	56173.30190	301.33375	0.45	+54.40884	0.45
Keck/MOSFIRE	56211.291625	301.3336420	0.33	+54.4088130	0.31
Keck/MOSFIRE	56442.5828353	301.3333410	0.36	+54.4086280	0.29

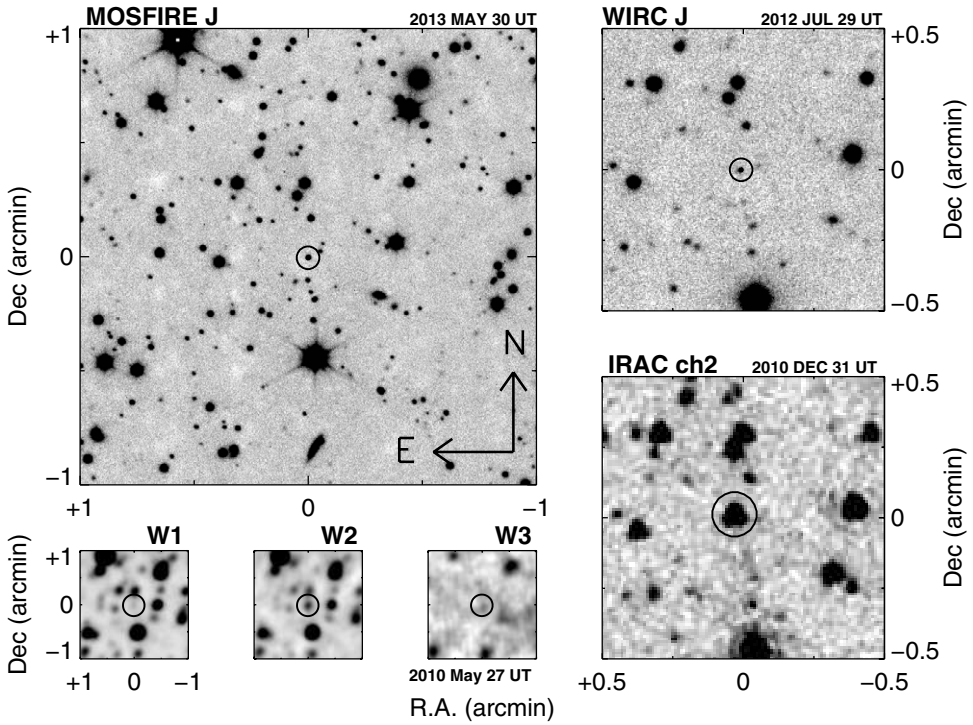

Figure 1. Finder chart collection centered on WISE 2005+5424. Images are labeled with the instrument, filter, and UT date of observation. WISE 2005+5424 is marked by a circle. A full list of our observations is provided in Table 2.

$W1 - W2$ color of WISE 2005+5424 results in red $J - W2$ and $H - W2$ colors, which are also consistent with a late-type T dwarf classification (see Figures 7 and 8 in Kirkpatrick et al. 2011).

2.5. MOSFIRE

The Multi-Object Spectrometer For Infra-Red Exploration (MOSFIRE; McLean et al. 2012) is a spectrometer and imager employed at the Cassegrain focus of the 10 m Keck I telescope at W. M. Keck Observatory. MOSFIRE provides imaging over a field of view of ∼6.′9 diameter with 0.″18 pix^{-1} sampling. The detector is a $2K \times 2K$ H2-RG HgCdTe array from Teledyne Imaging Sensors with low dark current and low noise (Kulas et al. 2012). WISE 2005+5424 was observed with MOSFIRE in a box9 dither pattern with 20.37s exposures and 3 coadds, for a total exposure time of ∼61 s per dither. The signal-to-noise ratio for WISE 2005+5424 in the final mosaic is ∼600. We were able to detect WISE 2005+5424 in single, sky-subtracted exposures with signal-to-noise ratios of ∼200, but require the full dither set to construct a quality sky flat. The MOSFIRE filters are on neither the 2MASS nor MKO system since they are optimized for spectroscopy. Characterization of the methane imaging technique and photometric calibration of MOSFIRE is underway (S. E. Logsdon et al., in preparation). The astrometric coordinates derived for WISE 2005+5424 are the median of the nine individual J-band exposures and the uncertainty is the standard deviation of the offset between 2MASS reference coordinates and corresponding detections in the MOSFIRE image.

2.6. OSIRIS

High resolution images of WISE 2005+5424 were taken on 2013 June 19 UT with the OH Suppressing Infra-Red Imaging Spectrograph (OSIRIS; Larkin et al. 2006) on the Keck I telescope. The OSIRIS imager has a fixed plate scale

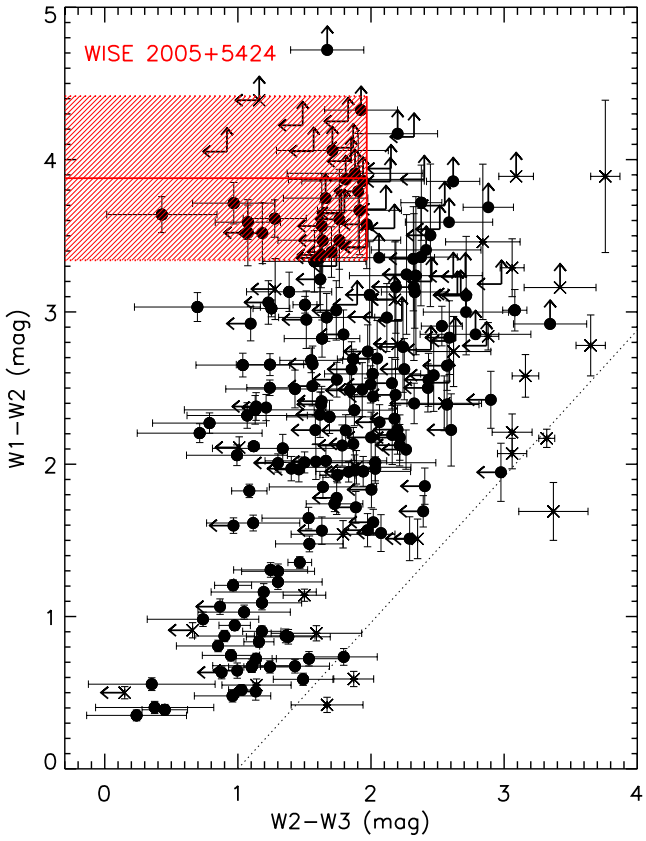

Figure 2. *WISE* $W1 - W2$ vs. $W2 - W3$ color–color diagram. A 1σ error box for the WISE 2005+5424 photometry is illustrated by the red shaded area. T dwarfs from Mace et al. (2013), Kirkpatrick et al. (2011, 2012), Mainzer et al. (2011), Cushing et al. (2011), and Burgasser et al. (2011) are marked with black circles and limit arrows. Interlopers are marked by black x's and limits. The dotted line identifies the $W1 - W2 > 0.96\,(W2 - W3) - 0.96$ selection criterion outlined by Kirkpatrick et al. (2011).

(A color version of this figure is available in the online journal.)

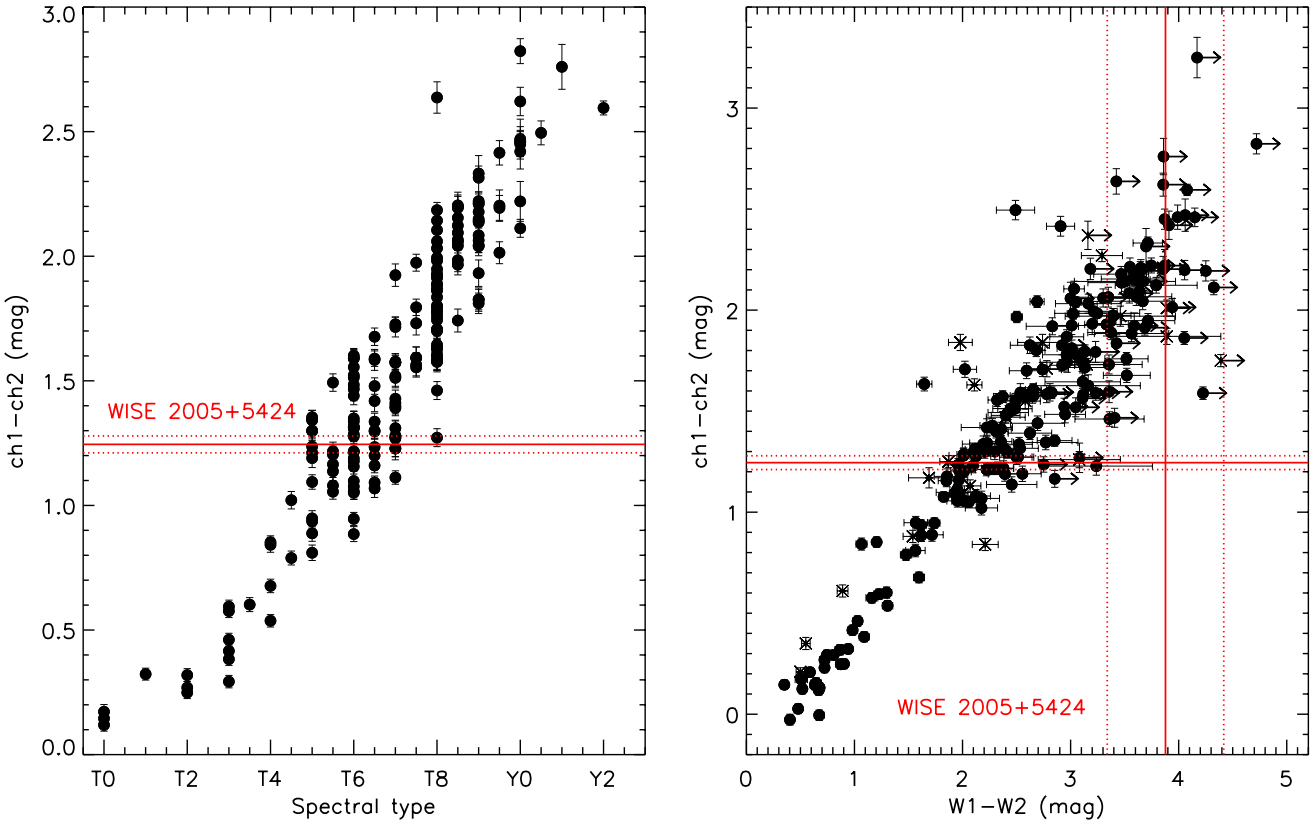

Figure 3. *Spitzer* $ch1 - ch2$ vs. spectral type and *WISE* $W1 - W2$ color. The symbols are the same as in Figure 2. *Spitzer* photometry constrains WISE 2005+5424 to spectral types between T5 and T8 and WISE 2005+5424 occupies a unique corner of the color–color diagram.

(A color version of this figure is available in the online journal.)

of 0.″02 pix^{-1} and a field of view of 20″. We used the $R = 14.1$ USNO B star 1444−0306431 (Monet et al. 2003) for the input of the Natural Guide Star (Wizinowich et al. 2000) wavefront sensor. Five images were taken in the *Hbb* filter (a broad-band *H* filter) with single frame exposure times of 120 s. WISE 2005+5424 has a FWHM of 0.″14 on the mosaic created from the five images. There are no obvious companions detected, nor does the PSF of WISE 2005+5424 differ significantly from other objects in the mosaic.

2.7. NIRSPEC

Employing the slit-viewing camera (SCAM) on the Near-Infrared Spectrometer (NIRSPEC; McLean et al. 1998, 2000) at Keck Observatory, we obtained a nodded pair of images of WISE 2005+5424. SCAM is a 256 × 256 HgCdTe array behind the NIRSPEC filter wheel that images a 46″ square field around the science slit. Astrometric measurements from SCAM utilized ten reference stars. Only four of the objects in the field were detected by 2MASS and coordinates for the remaining reference stars were taken from our deeper MOSFIRE images. Position uncertainties are estimated as the seeing (0.″45) at the time of observation.

3. SPECTROSCOPY

With NIRSPEC we observed WISE 2005+5424 in the medium-resolution mode with the *Y*-band (N1) and *J*-band (N3) filters. An *H*-band spectrum of WISE 2005+5424 was obtained with MOSFIRE in spectroscopic mode. Figure 5 shows the *Y*-, *J*-, and *H*-band NIRSPEC and MOSFIRE spectra along with

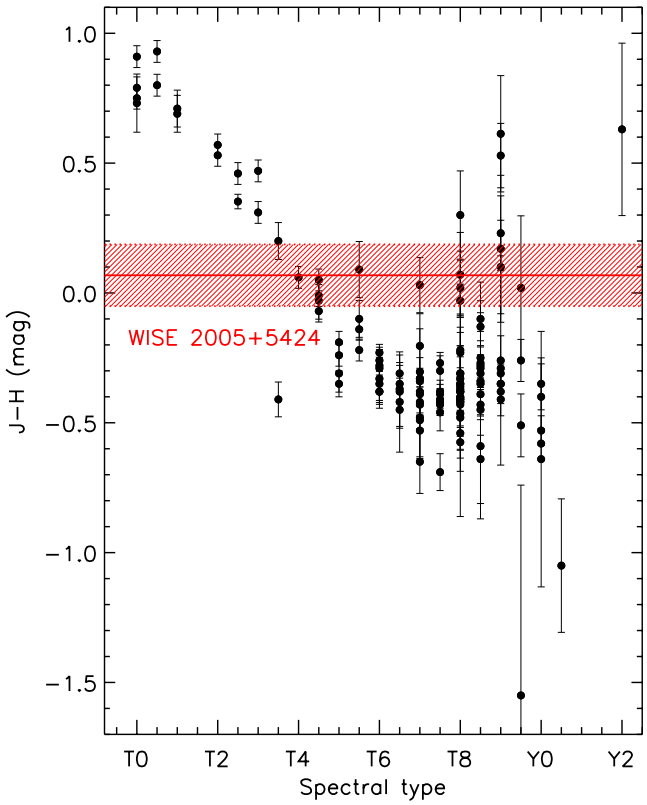

Figure 4. Palomar/WIRC $(J - H)_{\rm MKO}$ color vs. spectral type. WISE 2005+5424 photometry encloses the shaded area, which is redder than most late-type T dwarfs. Data points are collected from the literature cited in Section 2.4.

(A color version of this figure is available in the online journal.)

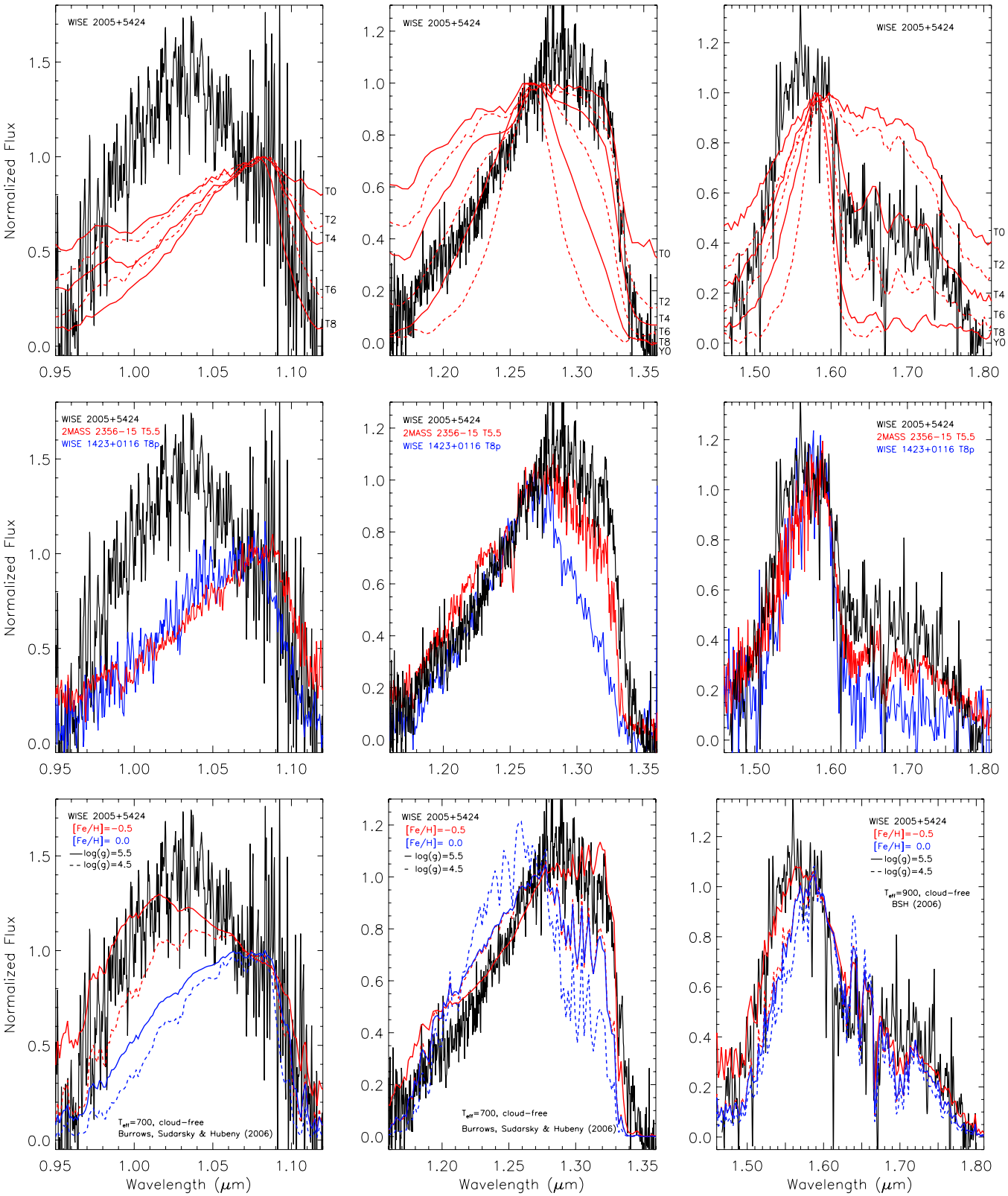

Figure 5. NIRSPEC *Y*- and *J*-band and MOSFIRE *H*-band spectra of WISE 2005+5424 (solid black lines) normalized at ∼1.08, 1.28, and 1.59 μm respectively. For comparison, the top row includes the T0, T2, T4, T6, T8, and Y0 spectral standards (red lines, labeled on the axis; Burgasser et al. 2006a; Cushing et al. 2011). The middle panels include the T5.5 dwarf 2MASS J23565477−1553111 (solid red line) and peculiar T8 dwarf WISE J142320.84+011638.0 (solid blue line). In the bottom row we include the best matching cloud-free models from Burrows et al. (2006) for the various log(g), [Fe/H], and $T_{\rm eff}$ values listed.

(A color version of this figure is available in the online journal.)

comparisons to observed and model T dwarf spectra (discussed in detail in Section 4.2).

3.1. NIRSPEC

On 2013 May 21 UT we observed WISE 2005+5424 in the *Y* band with the 0.″38 slit ($R \sim 2350$). Six 600 s exposures were reduced with the publicly available REDSPEC package with modifications to remove residuals from the sky-subtracted pairs prior to 1D spectral extraction. The wavelength solution was derived from OH sky-lines. The A0 standard HD 199217 was observed at a similar airmass as the target for telluric correction of the spectrum. In the *J* band we used the 0.″57 slit ($R \sim 1400$) on three different epochs with two different A0 standards; 2012 June 08 UT (HD 199217), 2012 September 06 UT (HD 199217), and 2012 September 25 UT (HD 205314). Comparison of arclamp and sky-line locations throughout each night show no offset between the first spectrum of WISE 2005+5424 and the last spectrum of the A0 standard and provides consistent wavelength calibrations. The combined spectrum is a compilation of 11 nod pairs (22×300 s exposures) for a total integration time of 6600 s. Final *J*-band wavelength solutions were derived from NeAr arc lamp spectra acquired before or after observations of WISE 2005+5424 and the A0 standards.

3.2. MOSFIRE

From the *WISE* and NIRSPEC/SCAM coordinates we derived an initial estimate of the proper motion for WISE 2005+5424. Using this proper motion, we updated the coordinates of WISE 2005+5424 and used the MOSFIRE Automatic GUI-based Mask Application (MAGMA)[6] to design a slitmask centered on WISE 2005+5424. An *H*-band spectrum was obtained on 2012 October 12 UT with a spectral resolution of $R \sim 3500$ for a 0.″7 slit width. Observations were made using a Nod2 (AB) pattern with exposure times of 120 s to minimize skyline saturation, resulting in 17 high-quality nod pairs and a total exposure time of 4080 s. For telluric correction we observed the A0 standard HD 199066 ($V = 9.10$) at five locations along a $15'' \times 0.''7$ slit with 12 s exposures. A modified version of the REDSPEC package was used for spectral extraction and telluric correction, and wavelength solutions made use of OH skylines.

4. ANALYSIS

4.1. The Companionship of WISE 2005+5424 and Wolf 1130

Wolf 1130 is a well known high-proper motion system (Wolf 1921; Ross 1939; Giclas et al. 1968; Luyten 1976; Gliese & Jahreiß 1991; van Leeuwen 2007) with $\mu_\alpha = -1.''163 \pm 0.''005$ yr^{-1} and $\mu_\delta = -0.''900 \pm 0.''004$ yr^{-1}. Parallax measurements of 59.4 ± 2.4 mas (Harrington & Dahn 1980), 61 ± 2 mas (van Altena et al. 1995), and 63.17 ± 3.82 mas (van Leeuwen 2007) place Wolf 1130 between 14.9 and 17.5 pc from the Sun. It is also a single-lined spectroscopic binary (Joy 1947; Gliese 1969; Stauffer & Hartmann 1986; Dawson & De Robertis 1998) with a radial velocity range of $\sim$240 km s^{-1} and a center of mass velocity $\gamma \approx -34$ km s^{-1} (Gizis 1998). From the parameters in Table 1 we derive UVW velocities for Wolf 1130, relative to the Sun, of -101 ± 7, -44 ± 2, and 33 ± 3, respectively. This is consistent with the old disk-halo membership requirements of Leggett (1992).

[6] Available at http://www2.keck.hawaii.edu/inst/mosfire/magma.html.

Additional constraints on the age of Wolf 1130 are provided by its metallicity and binarity. Gizis (1997) presents optical spectroscopy, along with CaH and TiO spectral indices (Reid et al. 1995), and derives a subdwarf M1.5 classification for Wolf 1130. Lépine et al. (2007) also classify it as a subdwarf on their expanded classification scheme. From a large sample of M dwarf *K*-band spectra, in which Wolf 1130 is the most iron-poor member, Rojas-Ayala et al. (2012) determine $T_{\rm eff} = 3483 \pm 17$ K, $[{\rm M/H}] = -0.45 \pm 0.12$ dex, and $[{\rm Fe/H}] = -0.64 \pm 0.17$ dex. Other [Fe/H] calculations in the literature are -0.80 dex (Woolf et al. 2009), -0.87 dex (Stauffer & Hartmann 1986), -0.89 dex (Bonfils et al. 2005), and -1.02 dex (Schlaufman & Laughlin 2010). Despite the presumed old age of Wolf 1130, Stauffer & Hartmann (1986) note Hα emission in their optical spectra, and Reid et al. (1995) and Gizis (1998) identify Hα and Hβ variability. The source of this hydrogen emission may be related to the $\sim$12 hr period of Wolf 1130 derived by Gizis (1998) in his single-lined orbital solution. Young et al. (1987) reason that M-dwarfs in binary systems with periods less than $\sim$5 days are agitated into producing Balmer line emission as a result of tidally increased rotational velocities. Indeed, Wolf 1130 has a large rotational velocity ($v \sin i \approx 15$–30 km s^{-1}; Stauffer & Hartmann 1986; Gizis 1998) relative to most other early-type M dwarfs ($v \sin i \leqslant 10$ km s^{-1}; Jenkins et al. 2009).

Combining his orbital solution with the lack of secondary spectral lines, and the fact that the Wolf 1130 photometry is consistent with other M subdwarfs, Gizis (1998) concludes that the companion is most likely a $\sim$0.35 $M_\odot$ helium white dwarf. Based on the calculations by Hansen & Phinney (1998) the age of Wolf 1130 is at least 2 Gyr, but more likely 10–15 Gyr. Furthermore, as the secondary component of Wolf 1130 lost mass and transitioned into a white dwarf, common envelope evolution may have forced the mass ratio of the system closer to unity and ensured the ejection of the envelope material (Ivanova et al. 2013). The ejection of the envelope would have reduced the separation of the sdM1.5+WD binary and produced the short period derived by Gizis (1998).

A number of imaging campaigns have searched for additional companions to Wolf 1130, but were either not deep enough to detect the much fainter WISE 2005+5424 component and/or not wide-field enough to enclose both objects. Jao et al. (2009) used the KPNO Mayall 4 m telescope and the United States Naval Observatory (USNO) speckle camera (Mason et al. 2006) to search for companions at 5500 ± 240 Å in only a $3'' \times 3''$ field. C.R.Gelino observed Wolf 1130 on 2005 August 01 UT with the Keck natural guide star adaptive optics in the K_s filter on the NIRC2 instrument. Short exposures and a $40'' \times 40''$ field of view excluded WISE 2005+5424 and didn't reveal the white dwarf component at the 50 mas scale. Riaz et al. (2006) presents *Spitzer* observations of Wolf 1130 made between 2004 October and 2006 March and also did not detect WISE 2005+5424 in their shallow IRAC and MIPS imaging at 3.6, 4.5, 5.8, 8, and 24 μm.

Fitting our astrometry with both the proper motion and parallax as free parameters, we derive a proper motion for WISE 2005+5424 of $\mu_\alpha = -1.''138 \pm 0.''102$ yr^{-1} and $\mu_\delta = -0.''988 \pm 0.''106$ yr^{-1}, which is the same as the published values for Wolf 1130 to within 1σ. Our position measurements are not precise enough to strongly constrain the parallax of WISE 2005+5424 and we derive an insignificant parallax of $0.''019 \pm 0.''096$. The astrometric measurements for WISE 2005+5424 are compiled in Table 2. Figure 6 illustrates the agreeable match in our astrometric fits when proper motion and parallax

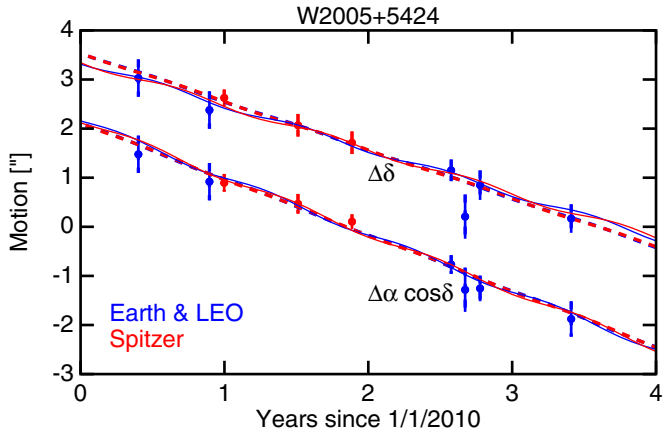

Figure 6. Astrometric fits for WISE 2005+5424. The blue curves and points are for ground-based or Low Earth Orbit observatories, while the red curves and points are for *Spitzer*. The dashed lines show the fit with proper motion and parallax as free parameters, while the lighter solid curves show the fit forced to match Wolf 1130. $\Delta\delta$ has been displaced by a constant for clarity.

(A color version of this figure is available in the online journal.)

are left as free parameters (dashed lines) or forced to be the same as Wolf 1130 (solid lines). The fit with parallax and proper motion as free parameters gives $\chi^2 = 6.72$ for 13 degrees of freedom, while the fit forced to match the motion of Wolf 1130 gives $\chi^2 = 8.07$ for 16 degrees of freedom. Based on the companionship criteria of Lépine & Bongiorno (2007, $\Delta X = ((\mu/0.15)^{-3.8}\Delta\theta\Delta\mu)^{1/2} < 1$) and Dupuy & Liu (2012, $\Delta\mu/\mu < 0.2$) it is unlikely that WISE 2005+5424 and Wolf 1130 ($\Delta X \approx 0.07$ and $\Delta\mu/\mu \approx 0.12$) are a chance alignment. Assuming that the distance to WISE 2005+5424 is the same as Wolf 1130 (15.83 ± 0.96 pc), from the current angular separation ($188\farcs5$) we calculate a projected separation of 2985 ± 181 AU. The orbital period at this distance is on the order of 200,000 yr. As discussed by Day-Jones et al. (2011, Section 3.1), a brown dwarf in a system slowly losing mass would migrate outward by to up to ~4 times its original distance. Before this migration WISE 2005+5424 would have been as close as 700 AU from Wolf 1130.

For a distance of 15.83 ± 0.96 pc, we derive the absolute H and $W2$ magnitudes that are given in Table 1. These values are shown in Figure 7 along with the late-type T dwarfs and magnitude-spectral type relations from Kirkpatrick et al. (2012). The absolute magnitudes we determine for WISE 2005+5424 are consistent with late-type T dwarfs, but slightly fainter than the T8 spectral type we assign in Section 4.2. The low luminosity of WISE 2005+5424 for its spectral type implies that it is not a close, equal mass binary with another brown dwarf since binaries are generally located above the absolute magnitude versus spectral type relations (Looper et al. 2008). Our Keck/OSIRIS H-band imaging, described in Section 2.6, does not reveal a companion to WISE 2005+5424 at $0\farcs14$ (~2.2 AU). Of course, we can not fully rule out the possibility of a fainter Y subdwarf companion (Leggett et al. 2013). The faintness of WISE 2005+5424 also implies that WISE 2005+5424 has a smaller radius and is older than other T8 dwarfs.

Burrows et al. (2003) model solivagant T dwarfs with temperatures between ~130 and 800 K with masses from 1 to 25 M_J and solar metallicities to show that the $J-H$, $J-W2$, and $H-W2$ colors redden as late-type T dwarfs age. This reddening is also seen in other models (Saumon & Marley 2008; Morley et al. 2012) and in the observed colors of late-type T dwarfs (Kirkpatrick et al. 2012; Leggett et al. 2013). Burrows et al. (2006) also consider non-solar metallicities for temperatures between 700 and 2200 K. The 3–6 μm flux of the 700 K models predict the reddest $J-W2$ and $H-W2$ colors for older objects with high surface gravities and low metallicities. Stephens et al.

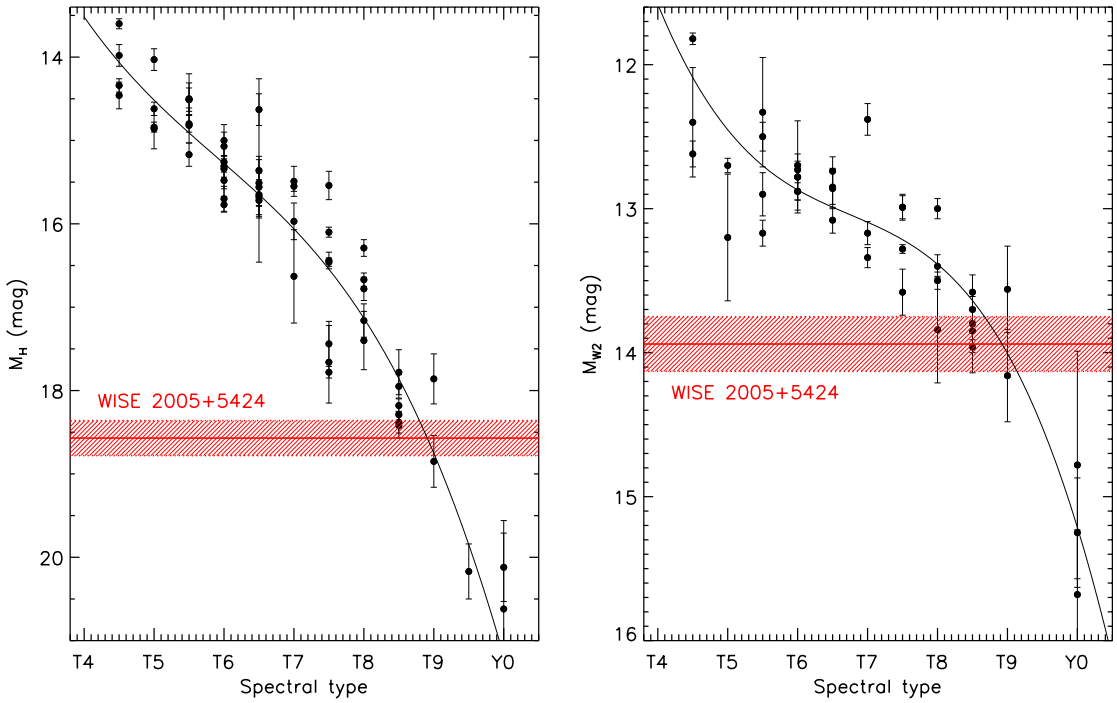

Figure 7. Absolute H and $W2$ magnitudes vs. spectral type (Figures 12 and 13, Kirkpatrick et al. 2012). The range for WISE 2005+5424 (assuming a distance of 15.83 pc) is shown by the shaded region. Both absolute magnitude ranges are below the trend lines at the T8 spectral type that we assign, which supports its subdwarf classification.

(A color version of this figure is available in the online journal.)

(2009) constrain the effective temperature of a T8 to between 600 and 900 K. WISE 2005+5424 displays the reddened colors associated with a late-type T subdwarf, which agrees with the age of Wolf 1130 of at least 2 Gyr (and likely 10–15 Gyr). Baraffe et al. (2003) predict that at 1 Gyr, a brown dwarf in our assumed range of $T_{\rm eff}$ would have a mass of $\sim$0.020 $M_{\odot}$ and radius 0.100 $R_{\odot}$. At 10 Gyr, a brown dwarf of this temperature would have a mass $\sim$0.050 $M_{\odot}$ and radius 0.079 $R_{\odot}$. Burrows et al. (2011) model brown dwarf radii and find that old, low-metallicity brown dwarfs are $\sim$10%–25% smaller than younger, solar metallicity brown dwarfs. If WISE 2005+5424 is old and metal-poor then it is likely small. This decreased size partially explains why the absolute magnitudes are fainter than we expect for the T8 spectral type.

4.2. Comparing WISE 2005+5424 to Observed and Synthetic Spectra

In Figure 5 we present *Y*-, *J*-, and *H*-band spectroscopy of WISE 2005+5424. Without significant overlap between the individual bands, and because of the low signal-to-noise of the spectra, we are not able to reliably flux calibrate the bands relative to each other. To produce a meaningful comparison we normalize each of our spectra at the standard flux peak for that band; *Y* ($\sim$1.08 μm), *J* ($\sim$1.28 μm), and *H* ($\sim$1.59 μm). The top panels of the figure show the T0, T2, T4, T6, and T8 spectral standards of Burgasser et al. (2006a)[7] and the Y0 standard (WISEP J173835.52+273258.9) defined by Cushing et al. (2011). The middle row compares our observed spectra to the T5.5 dwarf 2MASS J23565477−1553111[8] (Burgasser et al. 2002, 2006a) and the peculiar T8 dwarf WISE J142320.84+011638.0 (BD +01°2920B; Pinfield et al. 2012; Mace et al. 2013). The 2MASS 2356−1553 spectra were published by McLean et al. (2003) and represent the mid-type T dwarf classification that some of our photometry imply. WISE 1423+0116 is the closest object of similar type to WISE 2005+5424 in the literature and the Magellan/FIRE spectrum from Mace et al. (2013) is used here for comparison. Discovered by Pinfield et al. (2012), WISE 1423+0116 is a companion to a G1 dwarf at $\sim$17.2 pc, which provides an inferred [Fe/H] = −0.36 ± 0.06 dex. Based on comparison to the model isochrones of Baraffe et al. (2003) they estimate $T_{\rm eff}$ = 680 ± 55 K and log(g) = 5.0 ± 0.3 dex for WISE 1423+0116. The bottom panels of Figure 5 present the cloud-free models from Burrows et al. (2006) with [Fe/H] = 0 and −0.5 dex and log(g) = 4.5 and 5.5 dex.

Our *Y*-band spectrum of WISE 2005+5424 shows the strongest hallmarks of low-metallicity. Comparison with the spectral standards reveals that the peak *Y*-band flux of WISE 2005+5424 has shifted from the standard peak location of $\sim$1.08 μm to $\sim$1.03 μm. As depicted in Figure 3 of Burgasser et al. (2006b), this shift and brightening at bluer wavelengths is a well predicted trait of low-metallicity T dwarfs. No other T dwarf in the literature shows this broad morphology, which makes a *Y*-band spectral type difficult to determine based on the spectral standards alone. The only feature that is consistent with the standards is the red wing of the *Y* band, which is most like a T8. Comparing the observed templates to WISE 2005+5424 we also see that WISE 1423+0116 is slightly brighter than 2MASS 2356−1553 between 1.00 and 1.06 μm, but much like WISE 2005+5424 in the red wing. Burrows et al. (2006) provide models only down to 700 K, which gives a good match to WISE 2005+5424. It is possible that lower temperature models may provide an even better match. In any case, the 700 K solar metallicity models shown in Figure 5 are similar to the observed templates, while the −0.5 dex metallicity models best match WISE 2005+5424.

Comparison of the WISE 2005+5424 *J*-band spectrum to the spectral standards and observed templates again emphasizes its uniqueness. The width of the *J*-band flux peak does not follow the smooth transition that defines the spectral sequence. The blue wing of the *J* band is distorted relative to the other T dwarfs, while the red wing contains the bulk of the flux. A similar *J*-band morphology was seen by Burningham et al. (2010a) and Burgasser et al. (2010) in the low-metallicity, high-gravity T7.5 dwarf SDSS J141624.08+134826.7B (although with different strengths, implying slight spectral variability of the feature on the timescale of about a month). Additionally, the K I doublet at 1.243 and 1.254 μm is seen in the T5.5 comparison spectrum but is absent for WISE 2005+5424. This is a distinct indicator of its low-temperature and/or high surface gravity (McLean et al. 2003). We do not decide on a spectral type for the *J*-band spectrum of WISE 2005+5424 and therefore give a range between T5 and T8. The same 700 K models from Burrows et al. (2006) demonstrate degeneracy between metallicity and gravity in the overlap between the low-gravity, low-metallicity (red dashed) case and the high-gravity, solar-metallicity (blue solid) one. It is only at the extremes that the *J* band can differentiate between the different model parameters. Just as in the *Y* band, WISE 2005+5424 is bracketed by the [Fe/H] = −0.5 dex models with log(g) = 4.5–5.5 dex at a temperature of 700 K. Higher temperature models produce wider *J* band fluxes and less agreement with WISE 2005+5424, but lower temperature models may provide a better match.

In the *H* band, WISE 2005+5424 shows fewer inconsistencies with the observed templates, but its continuum is most like a mid-type T dwarf, rather than the late-type that the other bands imply. The best matching Burrows et al. (2006) models have an effective temperature of 900 K and show the same gravity-metallicity degeneracies as the *J* band. However, WISE 2005+5424 is well matched to the [Fe/H] = −0.5 dex and log(g) = 5.5 dex model.

From our model comparisons, we estimate the spectral type of WISE 2005+5424 as T8, with an effective temperature between 600 and 900 K. This is consistent with what Stephens et al. (2009) derives for a T8, but is at the limits of that study. Although the *H*-band spectrum is better matched with higher temperature models and an earlier spectral type, these characteristics would be completely inconsistent with the other spectroscopic bands and with much of our photometry. Burningham et al. (2008) identify ULAS J101721.40+011817.9 as a peculiar T8 that is similar to WISE 2005+5424 since it is more like a T6 in the *H* and *K* bands. Through comparison to the BT-Settl models (Allard et al. 2003), but without a *Y*-band spectrum to constrain metallicity well, they estimate a large surface gravity (log(g) = 5–5.5 dex) and a wide range of ages between 1.6 and 15 Gyr. However, none of the solar metallicity models they use provide an especially good fit to the spectrum.

4.3. Identifying T Dwarfs with Color Indices Similar to WISE 2005+5424

The location of WISE 2005+5424 in *WISE* color space is unusual, but not unique. The standout objects in Figure 2 have $W2 - W3 \leqslant 1.3$ and are WISE J000517.48+373720.5 (T9), WISE J045853.89+643452.5

[7] Spectra from the SpeX Prism Spectral Library; maintained by Adam Burgasser.

[8] Spectra from the BDSS; McLean et al. (2003, 2007); http://bdssarchive.org/.

(T8.5), WISE J062309.94−045624.6 (T8), WISE J115013.85+630241.5 (T8), WISE J121756.90+162640.8 (T9), and WISE J152305.10+312537.6 (T6.5p) (Kirkpatrick et al. 2011; Mace et al. 2013). This subset includes WISE 0458+6434, a T8.5+T9 binary (Mainzer et al. 2011; Gelino et al. 2011; Burgasser et al. 2012), and WISE 1523+3125, a peculiar T6.5 dwarf that Mace et al. (2013) identifies as having the same low-metallicity hallmarks as 2MASS J09373487+2931409 (T6pec; Burgasser et al. 2002).

Figure 3 demonstrates that in *Spitzer* and *WISE* colors WISE 2005+5424 is only coincident with WISE J174556.65+645933.8 (T7), WISE J190903.16−520433.5 (T5.5), WISE J223729.52−061434.4 (T5), and WISE J233543.79+422255.2 (T7) (Kirkpatrick et al. 2011; Mace et al. 2013). However, none of these objects are noted as peculiar in the limited near-IR photometry and spectroscopy currently compiled for them. The primary difference between the *WISE* and *Spitzer* passbands, as they pertain to late-type brown dwarfs (Figure 2, Mainzer et al. 2011), is that the cutoff for the *Spitzer* $ch2$ band is at $\sim$5 μm and the $W2$ cutoff is closer to $\sim$5.2 μm. Approximately 10%–15% of the emergent flux is in this Δ0.2 μm window, which produces a slightly redder $W1-W2$ color relative to $ch1-ch2$ (Leggett et al. 2013) regardless of the impacts of non-equilibrium chemistry (Saumon et al. 2007; Hubeny & Burrows 2007) and sulfide or iron/silicate clouds at wavelengths just below $\sim$5 μm (Morley et al. 2012).

Recently, Burningham et al. (2013) presented a new sample of color and proper-motion selected T dwarfs from the UKIDSS Large Area Survey. Figure 12 of that work presents the $J-H$ versus $H-ch2$ colors of T dwarf benchmarks and the compilation of T dwarf colors from Leggett et al. (2010a). We expand upon that plot in Figure 8 of this paper, which shows the $J-H$ versus $H-ch2$ color-space for T and Y dwarfs, by including additional photometry for objects in Figure 4. This expanded sample indicates that there is a well defined sequence for the bulk of the population, but that there are also distant outliers. The general trend toward bluer $J-H$ colors as a result of significant methane absorption in the H band is a well known feature of the T dwarf sequence. At later spectral types, which corresponds to redder $H-ch2$ colors and lower effective temperatures, the dispersion does increase and the late-type T dwarfs begin to turn slightly redward. With the exception of WISE J154214.00+223005.2 and WISE J182831.08+265037.7 the Y dwarfs are distinctly redder than the T dwarfs in $H-ch2$ and bluer in $J-H$.

WISE 1542+2230 was discovered by Mace et al. (2013) and classified as a T9.5 from a *Hubble Space Telescope* Wide Field Camera 3 (Kimble et al. 2008) spectrum. The median flux spectral indices are mostly consistent with a T9.5 but the J-narrow index is closer to a Y0 than a T9.5 (Mace et al. 2013). Additional photometry of this source would improve its placement in Figure 8 and reveal if it is actually bluer in $J-H$ than most Y dwarfs. WISE 1828+2650 was discovered by Cushing et al. (2011) and initially classified, based on its equal-height J- and H-band peaks, as a >Y0 dwarf. Kirkpatrick et al. (2012) further expanded the Y dwarf population and with the introduction of the Y1 spectral type moved WISE 1828+2650 to a later type of $\geqslant$Y2. WISE 1828+2650 is still a distant outlier in Figure 8. Its $H-ch2$ color is consistent with the latest Y dwarf classification that it has been given, but its $J-H$ color is only matched by the largest T dwarf outliers.

Table 3 lists the T dwarfs later than T6 that have $J-H$ colors greater than −0.2 and less than −0.5. With $J-H=0.068\pm0.119$, WISE 2005+5424 is adjacent to 13 other red outliers that are primarily from *WISE* (Kirkpatrick et al. 2011; Mace et al. 2013; Thompson et al. 2013). The exception is the T8 dwarf ULASJ095047.28+011734.3, which was first presented by Leggett et al. (2012). Burningham et al. (2013) identify ULAS J0950+0117 as a companion to LHS 6176, which is an M4 dwarf with [Fe/H] = −0.30 ± 0.1. The red outliers discovered with *WISE* were classified from Keck/NIRSPEC J-band spectra or Magellan/FIRE near-IR spectra. In the cases where J-band spectra were used for classification, identification of peculiar objects is not possible without broader wavelength coverage. As discussed in Mace et al. (2013, Section 5 and Appendix), a number of the late-type T dwarfs have a larger Y/J index and a smaller K/J index than the spectral standards defined by Burgasser et al. (2006a) and Cushing et al. (2011). Although these objects all have bluer $Y-J$ and $J-K$ colors (inferred from the Y/J and K/J indices), they were not classified as peculiar since they were all observed with the same instrument (Magellan/FIRE) and the possibility of an instrumental bias was too strong to ignore. The addition of $J-H$ colors in identifying these objects as outliers implies that the objects listed in Table 3 should also be classified as peculiar,

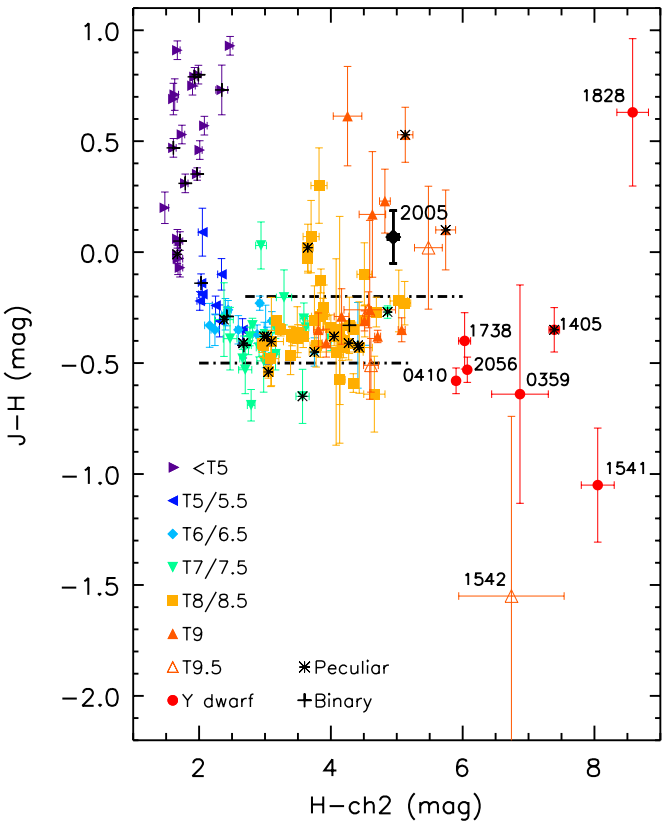

Figure 8. $J-H$ vs. $H-ch2$ color–color diagram. Data points are on the MKO filter system and collected from the literature referenced in Section 2.4. Various colored symbols differentiate the spectral type bins. Peculiar or binary objects in the literature are marked additionally. We have marked by name WISE 2005+5424 (this paper), WISE 1542+2230 (T9.5; Mace et al. 2013), and the Y dwarfs WISE 0359−5401 (Y0), WISE 0410+1502 (Y0), WISE 1405+5534 (Y0p), WISE 1541−2250 (Y0.5), WISE 1738+2732 (Y0), WISE 1828+2650 ($\geqslant$Y2), and WISE 2056+1459 (Y0) with photometry from Cushing et al. (2011), Kirkpatrick et al. (2012), and Leggett et al. (2013). Old, metal-poor late-type T dwarfs like WISE 2005+5424 have $J-H>-0.2$, while young, metal-rich late-type T dwarfs have $J-H<-0.5$ (dash-dotted lines).

(A color version of this figure is available in the online journal.)

Table 3
Late-type T Dwarf $J-H$ Color Outliers

Object	Spectral Type	$J-H$	$H-ch2$	Reference
Red: $J-H > -0.2$				
WISE J000517.48+373720.5	T9	0.230 ± 0.144	4.820 ± 0.082	4
WISE J032120.91−734758.8	T8	0.070 ± 0.163	3.700 ± 0.122	4
WISE J041358.14−475039.3	T9	0.170 ± 0.283	4.630 ± 0.201	4
WISE J054047.00+483232.4	T8.5	-0.130 ± 0.054	3.850 ± 0.054	4
WISE J075946.98−490454.0	T8	-0.030 ± 0.064	3.649 ± 0.044	3, 4
WISE J081117.81−805141.3	T9.5:	0.020 ± 0.277	5.480 ± 0.211	4
ULAS J095047.28+011734.3	T8p	0.020 ± 0.106	3.650 ± 0.082	5, 4, 6
WISE J104245.23−384238.3	T8.5	-0.100 ± 0.142	4.508 ± 0.112	3, 4
WISE J113949.24−332425.1	T7	0.030 ± 0.106	2.940 ± 0.082	2
WISE J144806.48−253420.3	T8	0.300 ± 0.170	3.820 ± 0.122	2
WISE J161441.46+173935.5	T9	0.613 ± 0.224	4.253 ± 0.217	3
WISE J200520.38+542433.9	T8p	0.068 ± 0.119	4.947 ± 0.081	1
WISE J213456.73−713744.5	T9p	0.100 ± 0.180	5.742 ± 0.151	3
WISE J232519.53−410535.0	T9p	0.529 ± 0.124	5.129 ± 0.116	3
Blue: $J-H < -0.5$				
ULAS J013939.77+004813.8	T7.5	-0.690 ± 0.071	2.790 ± 0.058	8, 9
CFBDS J030135.11−161418.0	T7p	-0.650 ± 0.122	3.570 ± 0.100	6, 7
CFBDS J092250.12+152741.4	T7	-0.530 ± 0.108	2.700 ± 0.100	6, 7
ULAS J101721.40+011817.9	T8p	-0.540 ± 0.028	3.050 ± 0.036	11, 9
WISE J154214.00+223005.2	T9.5	-1.550 ± 0.810	6.740 ± 0.800	4
WISE J161705.74+180714.1	T8	-0.575 ± 0.112	4.137 ± 0.080	10, 3
WISE J180435.37+311706.4	T9.5:	-0.510 ± 0.121	4.608 ± 0.112	3
WISE J181210.85+272144.3	T8.5:	-0.640 ± 0.171	4.660 ± 0.161	10, 3, 4
Wolf 940B	T8.5	-0.590 ± 0.042	4.340 ± 0.042	12, 13

References. (1) This paper; (2) Thompson et al. 2013; (3) Kirkpatrick et al. 2011; (4) Mace et al. 2013; (5) Leggett et al. 2012; (6) Burningham et al. 2013; (7) Albert et al. 2011; (8) Chiu et al. 2008; (9) Leggett et al. 2010a; (10) Burgasser et al. 2011; (11) Burningham et al. 2008; (12) Burningham et al. 2009; (13) Leggett et al. 2010b.

and that there is not an inherent bias in the FIRE observations or reductions from Mace et al. (2013).

On the opposite side of the $J-H$ color sequence there are nine blue outliers, which are listed in Table 3. Albert et al. (2011) discuss the peculiar T7 dwarf CFBDS J030135.11−161418.0 as an extremely red ($H-K_s = 0.92 \pm 0.12$) outlier in Figure 7 of that paper. CFBDS J0301−1614 is also a red outlier in their $J-K_s$ color and a blue outlier in $J-H$. Through comparisons to BT-Settl models, Albert et al. (2011) identify CFBDS J0301−1614 as exhibiting either low gravity ($\log(g) = 3.5$–4.0) or high-metallicity. These are both signs of extreme youth. WISE J161705.74+180714.1 and WISE J181210.85+272144.3 were presented by Burgasser et al. (2011) as low-gravity, late-type T dwarfs, with WISE 1617+1807 matching cool (∼600 K) and cloudy Saumon & Marley (2008) models while WISE 1812+2721 looks nearly identical to Wolf 940B. Wolf 940B is estimated as an object of intermediate gravity and age (Leggett et al. 2010b). However, Burgasser et al. (2011) derive a different mass and age for WISE 1812+2721 that is very similar to WISE 1617+1807. These differences underscore the difficulties and inconsistencies in constraining solivagant brown dwarf properties with atmospheric models alone. The enigmatic T8 dwarf ULAS J101721.40+011817.9 (discussed in Section 4.2) is also in this group of blue $J-H$ outliers, despite having some similar features to WISE 2005+5424.

From the general properties of the $J-H$ outliers it is tempting to say that T dwarfs with $J-H \leqslant -0.5$ are young and low-mass. Also, $J-H$ colors greater than -0.2 appear to correlate with high-gravity, low-metallicity and old age. Yet there are exceptions to each of these categories and the influence of binarity, clouds, and non-equilibrium chemistry could also produce these distant outliers. For example, Burningham et al. (2013) report $J-H = -0.38 \pm 0.04$ for ULAS J0950+0117, which is below the red-outlier requirement of -0.2, while Palomar/WIRC photometry from Mace et al. (2013) provides the 0.020 ± 0.106 color that we use to make our selection. Additionally, the UKIDSS photometry listed in Mace et al. (2013) produces a color between these two values of $J-H = -0.2 \pm 0.15$. However, it is unclear if the variability in these colors is real and only photometric monitoring can provide complete verification.

There are also young and old benchmarks that fall within the bulk $J-H$ color sequence and are not selected by the criteria that we outline. These include the young T8.5 dwarf Ross 458C ($J-H = -0.36 \pm 0.03$; Goldman et al. 2010; Burningham et al. 2011) and the old T8 dwarf WISE J142320.84+011638.0 ($J-H = -0.41 \pm 0.08$; Mace et al. 2013; Pinfield et al. 2012) that we use for spectral comparison in Section 4.2. The addition of WISE 2005+5424, which has an inferred metallicity of $[\mathrm{Fe/H}] = -0.64 \pm 0.17$, to the group of red $J-H$ outliers makes a compelling argument that this group at least partially represents the low-metallicity T dwarf population. Additionally, the position of WISE 1828+2650 in Figure 8 argues that its distance from the other Y dwarfs may be a symptom of a characteristically low-metallicity in addition to a low temperature (see Section 6.6 of Burningham et al. 2013 for additional discussion).

5. CONCLUSIONS

The unique spectral features of WISE J200520.38+542433.9 make spectral classification against the standards difficult, but photometric colors and 600 to 900 K models with log(g) = 5.0–5.5 dex and [Fe/H] = −0.5 dex are in general agreement with near-infrared spectra. Photometry and spectroscopy of WISE 2005+5424 support its classification as a T8 subdwarf with common proper motion to the single-lined spectroscopic sdM1.5+WD binary Wolf 1130. Based on this companionship, WISE 2005+5424 has an inferred distance of 15.83 ± 0.96 pc and a metallicity of [Fe/H] = −0.64 ± 0.17. Hallmarks of high-gravity and low-metallicity are identified in our photometric and spectroscopic analysis. As the sample of late-type brown dwarf benchmarks is expanded to include more extreme temperatures, ages, metallicities, and gravities we can develop improved comprehensive models. It is only through direct comparison of observational data with these well constrained models that we can fully understand the bulk of the solivagant population.

This publication makes use of data products from the *Wide-field Infrared Survey Explorer*, which is a joint project of the University of California (UC), Los Angeles, and the Jet Propulsion Laboratory (JPL)/California Institute of Technology (Caltech), funded by the National Aeronautics and Space Administration. We thank the Infrared Processing and Analysis Center (IRAC) at Caltech for funds provided by the Visiting Graduate Fellowship for G.N.M. This publication also makes use of data products from 2MASS. 2MASS is a joint project of the University of Massachusetts and IPAC/Caltech, funded by the National Aeronautics and Space Administration and the National Science Foundation (NASA). This research has made use of the NASA/IPAC Infrared Science Archive (IRSA), which is operated by JPL, Caltech, under contract with NASA. Our research has benefited from the M, L, and T dwarf compendium housed at http://DwarfArchives.org, whose server was funded by a NASA Small Research Grant, administered by the American Astronomical Society. The Brown Dwarf Spectroscopic Survey (BDSS) is hosted by UCLA and provided an essential comparison library for our moderate-resolution spectroscopy. This research has benefited from the SpeX Prism Spectral Libraries, maintained by Adam Burgasser at http://pono.ucsd.edu/∼adam/browndwarfs/spexprism. We are also indebted to the SIMBAD database, operated at CDS, Strasbourg, France. This work is based in part on observations made with the *Spitzer Space Telescope*, which is operated by JPL, Caltech, under a contract with NASA. Support for this work was provided by NASA through an award issued to program 70062 by JPL/Caltech. This work is also based in part on observations made with the NASA/ESA *Hubble Space Telescope*, obtained at the Space Telescope Science Institute (STScI), which is operated by the Association of Universities for Research in Astronomy, Inc., under NASA contract NAS 5-26555. These observations are associated with program 12330. Support for program 12330 was provided by NASA through a grant from the STScI. The Keck/OSIRIS observations were supported by a NASA Keck PI Data Award, administered by the NASA Exoplanet Science Institute. The spectroscopic data presented herein were obtained at the Keck Observatory, which is operated as a scientific partnership among Caltech, UC and NASA. The Observatory was made possible by the generous financial support of the W.M. Keck Foundation. In acknowledgement of our observing time at Keck we further wish to recognize the very significant cultural role and reverence that the summit of Mauna Kea has always had within the indigenous Hawaiian community. We are most fortunate to have the opportunity to conduct observations from this mountain. We thank the anonymous referee for detailed and thoughtful recommendations to improve this paper prior to publication.

REFERENCES

Albert, L., Artigau, É., Delorme, P., et al. 2011, AJ, 141, 203
Allard, F., Guillot, T., Ludwig, H.-G., et al. 2003, in IAU Symp. 211, Brown Dwarfs, ed. E. Martín (San Francisco, CA: ASP), 325
Baraffe, I., Chabrier, G., Barman, T. S., Allard, F., & Hauschildt, P. H. 2003, A&A, 402, 701
Bonfils, X., Delfosse, X., Udry, S., et al. 2005, A&A, 442, 635
Burgasser, A. J., Burrows, A., & Kirkpatrick, J. D. 2006b, ApJ, 639, 1095
Burgasser, A. J., Cushing, M. C., Kirkpatrick, J. D., et al. 2011, ApJ, 735, 116
Burgasser, A. J., Geballe, T. R., Leggett, S. K., Kirkpatrick, J. D., & Golimowski, D. A. 2006a, ApJ, 637, 1067
Burgasser, A. J., Gelino, C. R., Cushing, M. C., & Kirkpatrick, J. D. 2012, ApJ, 745, 26
Burgasser, A. J., Kirkpatrick, J. D., Brown, M. E., et al. 2002, ApJ, 564, 421
Burgasser, A. J., Kirkpatrick, J. D., Cutri, R. M., et al. 2000, ApJL, 531, L57
Burgasser, A. J., Kirkpatrick, J. D., & Lowrance, P. J. 2005, AJ, 129, 2849
Burgasser, A. J., Looper, D., & Rayner, J. T. 2010, AJ, 139, 2448
Burningham, B., Cardoso, C. V., Smith, L., et al. 2013, MNRAS, 433, 457
Burningham, B., Leggett, S. K., Homeier, D., et al. 2011, MNRAS, 414, 3590
Burningham, B., Leggett, S. K., Lucas, P. W., et al. 2010a, MNRAS, 404, 1952
Burningham, B., Pinfield, D. J., Leggett, S. K., et al. 2008, MNRAS, 391, 320
Burningham, B., Pinfield, D. J., Leggett, S. K., et al. 2009, MNRAS, 395, 1237
Burningham, B., Pinfield, D. J., Lucas, P. W., et al. 2010b, MNRAS, 406, 1885
Burrows, A., Heng, K., & Nampaisarn, T. 2011, ApJ, 736, 47
Burrows, A., Sudarsky, D., & Hubeny, I. 2006, ApJ, 640, 1063
Burrows, A., Sudarsky, D., & Lunine, J. I. 2003, ApJ, 596, 587
Chiu, K., Liu, M. C., Jiang, L., et al. 2008, MNRAS, 385, L53
Cushing, M. C., Kirkpatrick, J. D., Gelino, C. R., et al. 2011, ApJ, 743, 50
Cutri, R. M., et al. 2012, yCat, 2311, 0
Dawson, P. C., & De Robertis, M. M. 1998, AJ, 116, 2565
Day-Jones, A. C., Pinfield, D. J., Ruiz, M. T., et al. 2011, MNRAS, 410, 705
Deacon, N. R., Liu, M. C., Magnier, E. A., et al. 2012a, ApJ, 755, 94
Deacon, N. R., Liu, M. C., Magnier, E. A., et al. 2012b, ApJ, 757, 100
Delorme, P., Willott, C. J., Forveille, T., et al. 2008, A&A, 484, 469
Dupuy, T. J., & Liu, M. C. 2012, ApJS, 201, 19
Fazio, G. G., Ashby, M. L. N., Barmby, P., et al. 2004, ApJS, 154, 39
Gelino, C. R., Kirkpatrick, J. D., Cushing, M. C., et al. 2011, AJ, 142, 57
Giclas, H. L., Burnham, R., & Thomas, N. G. 1968, LowOB, 7, 67
Gizis, J. E. 1997, AJ, 113, 806
Gizis, J. E. 1998, AJ, 115, 2053
Gliese, W. 1969, VeARI, 22, 1
Gliese, W., & Jahreiß, H. 1991, The Astronomical Data Center CD-ROM: Selected Astronomical Catalogs, Vol. I, ed. L. E. Brotzmann & S. E. Gesser (Greenbelt, MD: NASA/Astronomical Data Center, Goddard Space Flight Center)
Goldman, B., Marsat, S., Henning, T., Clemens, C., & Greiner, J. 2010, MNRAS, 405, 1140
Hansen, B. M. S., & Phinney, E. S. 1998, MNRAS, 294, 557
Harrington, R. S., & Dahn, C. C. 1980, AJ, 85, 454
Hubeny, I., & Burrows, A. 2007, ApJ, 669, 1248
Ivanova, N., Justham, S., Chen, X., et al. 2013, A&ARv, 21, 59
Jao, W.-C., Mason, B. D., Hartkopf, W. I., Henry, T. J., & Ramos, S. N. 2009, AJ, 137, 3800
Jenkins, J. S., Ramsey, L. W., Jones, H. R. A., et al. 2009, ApJ, 704, 975
Joy, A. H. 1947, ApJ, 105, 96
Kimble, R. A., MacKenty, J. W., O'Connell, R. W., & Townsend, J. A. 2008, Proc. SPIE, 7010, 43
Kirkpatrick, J. D., Cushing, M. C., Gelino, C. R., et al. 2011, ApJS, 197, 19
Kirkpatrick, J. D., Gelino, C. R., Cushing, M. C., et al. 2012, ApJ, 753, 156
Kulas, K. R., McLean, I. S., & Steidel, C. C. 2012, Proc. SPIE, 8453, 1S
Larkin, J., Barczys, M., Krabbe, A., et al. 2006, Proc. SPIE, 6269, 42
Lawrence, A., Warren, S. J., Almaini, O., et al. 2007, MNRAS, 379, 1599
Leggett, S. K. 1992, ApJS, 82, 351
Leggett, S. K., Burningham, B., Saumon, D., et al. 2010a, ApJ, 710, 1627
Leggett, S. K., Morley, C. V., Marley, M. S., et al. 2013, ApJ, 763, 130
Leggett, S. K., Saumon, D., Burningham, B., et al. 2010b, ApJ, 720, 252
Leggett, S. K., Saumon, D., Marley, M. S., et al. 2012, ApJ, 748, 74

Lépine, S., & Bongiorno, B. 2007, AJ, 133, 889
Lépine, S., Rich, R. M., & Shara, M. M. 2007, ApJ, 669, 1235
Liu, M. C., Leggett, S. K., & Chiu, K. 2007, ApJ, 660, 1507
Looper, D. L., Gelino, C. R., Burgasser, A. J., & Kirkpatrick, J. D. 2008, ApJ, 685, 1183
Lucas, P. W., Hoare, M. G., Longmore, A., et al. 2008, MNRAS, 391, 136
Luhman, K. L., Burgasser, A. J., & Bochanski, J. J. 2011, ApJL, 730, L9
Luhman, K. L., Patten, B. M., Marengo, M., et al. 2007, ApJ, 654, 570
Luyten, W. J. 1976, A Catalogue of Stars with Proper Motions Exceeding 0.5″ Annually (Minneapolis: Univ. Minnesota Press), (LHS)
Mace, G. N., Kirkpatrick, J. D., Cushing, M. C., et al. 2013, ApJS, 205, 6
Mainzer, A., Cushing, M. C., Skrutskie, M., et al. 2011, ApJ, 726, 30
Mason, B. D., Hartkopf, W. I., Wycoff, G. L., & Holdenried, E. R. 2006, AJ, 132, 2219
McCaughrean, M. J., Close, L. M., Scholz, R.-D., et al. 2004, A&A, 413, 1029
McLean, I. S., Becklin, E. E., Bendiksen, O., et al. 1998, Proc. SPIE, 3354, 566
McLean, I. S., Graham, J. R., Becklin, E. E., et al. 2000, Proc. SPIE, 4008, 1048
McLean, I. S., McGovern, M. R., Burgasser, A. J., et al. 2003, ApJ, 596, 561
McLean, I. S., Prato, L., McGovern, M. R., et al. 2007, ApJ, 658, 1217
McLean, I. S., Steidel, C. C., Epps, H. W., et al. 2012, Proc. SPIE, 8446, 0J
Monet, D. G., Levine, S. E., Canzian, B., et al. 2003, AJ, 125, 984
Morley, C. V., Fortney, J. J., Marley, M. S., et al. 2012, ApJ, 756, 172
Mugrauer, M., Seifahrt, A., Neuhäuser, R., & Mazeh, T. 2006, MNRAS, 373, L31
Murray, D. N., Burningham, B., Jones, H. R. A., et al. 2011, MNRAS, 414, 575
Nakajima, T., Oppenheimer, B. R., Kulkarni, S. R., et al. 1995, Natur, 378, 463
Pinfield, D. J., Burningham, B., Lodieu, N., et al. 2012, MNRAS, 422, 1922
Pinfield, D. J., Burningham, B., Tamura, M., et al. 2008, MNRAS, 390, 304
Pinfield, D. J., Jones, H. R. A., Lucas, P. W., et al. 2006, MNRAS, 368, 1281
Reid, I. N., Hawley, S. L., & Gizis, J. E. 1995, AJ, 110, 1838
Riaz, B., Mullan, D. J., & Gizis, J. E. 2006, ApJ, 650, 1133
Rojas-Ayala, B., Covey, K. R., Muirhead, P. S., & Lloyd, J. P. 2012, ApJ, 748, 93
Rosenthal, E. D., Gurwell, M. A., & Ho, P. T. P. 1996, Natur, 384, 243
Ross, F. E. 1939, AJ, 48, 163
Saumon, D., & Marley, M. S. 2008, ApJ, 689, 1327
Saumon, D., Marley, M. S., Leggett, S. K., et al. 2007, ApJ, 656, 1136
Schlaufman, K. C., & Laughlin, G. 2010, A&A, 519, A105
Scholz, R.-D., McCaughrean, M. J., Lodieu, N., & Kuhlbrodt, B. 2003, A&A, 398, L29
Simons, D. A., & Tokunaga, A. 2002, PASP, 114, 169
Skrutskie, M. F., Cutri, R. M., Stiening, R., et al. 2006, AJ, 131, 1163
Stauffer, J. R., & Hartmann, L. W. 1986, ApJS, 61, 531
Stephens, D. C., Leggett, S. K., Cushing, M. C., et al. 2009, ApJ, 702, 154
Thompson, M. A., Kirkpatrick, J. D., Mace, G. N., et al. 2013, PASP, 125, 809
Tinney, C. G., Burgasser, A. J., Kirkpatrick, J. D., & McElwain, M. W. 2005, AJ, 130, 2326
Tokunaga, A. T., Simons, D. A., & Vacca, W. D. 2002, PASP, 114, 180
van Altena, W. F., Lee, J. T., & Hoffleit, E. D. 1995, The General Catalogue of Trigonometric Stellar Parallaxes (New Haven, CT: Yale University Observatory)
van Leeuwen, F. 2007, A&A, 474, 653
Werner, M. W., Roellig, T. L., Low, F. J., et al. 2004, ApJS, 154, 1
Wilson, J. C., Eikenberry, S. S., Henderson, C. P., et al. 2003, Proc. SPIE, 4841, 451
Wilson, J. C., Kirkpatrick, J. D., Gizis, J. E., et al. 2001, AJ, 122, 1989
Wizinowich, P., Acton, D. S., Shelton, C., et al. 2000, PASP, 112, 315
Wolf, M. 1921, AN, 213, 31
Woolf, V. M., Lépine, S., & Wallerstein, G. 2009, PASP, 121, 117
Wright, E. L., Eisenhardt, P. R. M., Mainzer, A. K., et al. 2010, AJ, 140, 1868
Wright, E. L., Skrutskie, M. F., Kirkpatrick, J. D., et al. 2013, AJ, 145, 84
York, D. G., Adelman, J., Anderson, J. E., Jr., et al. 2000, AJ, 120, 1579
Young, A., Sadjadi, S., & Harlan, E. 1987, ApJ, 314, 272